Biochimica et Biophysica Acta, 646 (1981) 334–343
Elsevier/North-Holland Biomedical Press

BBA 79363

FLUORESCENCE POLARIZATION STUDY OF HUMAN ERYTHROCYTE MEMBRANES WITH 1-PHENYL-3-(2-NAPHTHYL)-2-PYRAZOLINE AS ORIENTATIONAL PROBE

J. EISINGER, N. BOENS * and J. FLORES

Bell Laboratories, 600 Mountain Avenue, Murray Hill, NJ 07974 (U.S.A.)

(Received December 2nd, 1980)
(Revised manuscript received April 13th, 1981)

Key words: Fluorescence polarization; Erythrocyte membrane; Phenylnaphthylpyrazoline

The emission and polarization spectra of 1-phenyl-3-(2-naphthyl)-2-pyrazoline (PNP) in various environments were studied. Compared to the widely used orientational membrane probe 1,6-diphenylhexatriene (DPH), PNP is five times less photolabile and since its fluorescence emission maximum is at longer wavelengths ($\lambda_{max} \sim 445$ nm), it is more suitable for use with intact erythrocytes. The limiting fluorescence anisotropy of PNP is 0.385. In erythrocyte ghosts, the steady-state emission anisotropy of PNP is a decreasing function of wavelength and its temperature dependence parallels that of DPH, dropping from 0.298 at 2°C to 0.185 at 38°C when averaged between 420 and 470 nm.

I. Introduction

Fluorescence probes are important tools for the study of the structure and dynamics of biological membranes and of their model systems and can provide information about membrane fluidity, the molecular motion and orientation of membrane components, changes in membrane potential, phase transitions and other membrane parameters [1–5]. In particular, fluorophores located in the phospholipid regions of membranes can be used to probe translational and rotational diffusion.

The latter application requires probes with high intrinsic emission anisotropies and nondegenerate transition moments for absorption and emission, as well as absorption and emission spectral properties which are compatible with the optical characteristics of the studied membrane systems.

This paper decribes a steady-state fluorescence and polarization study using a new lipid soluble probe, 1-phenyl-3-(2-naphthyl)-2-pyrazoline (PNP), in propylene glycol, phospholipid vesicles, detergent micelles and embedded in human erythrocyte membranes.

II. Instrumentation, Materials and Methods

1. Materials

The materials for the synthesis of the fluorescent probe were purchased from Aldrich Chemical Corp. and were used as received. De-ionized water was distilled twice before use in the experiments with phospholipid vesicles and ghosts. Ammonyx-LO (30% w/v) (Onyx Company, NJ) was used without further purification to prepare 2% aqueous solutions. Alumina (neutral-activity grade I) was obtained from Camag (Switzerland).

* Present address: Katholieke Universiteit Leuven, Celestijnenlaan 200F, B-3030 Heverlee, Belgium

Abbreviations: DPH, 1,6-diphenylhexatriene; DPPC, β,γ-dipalmitoyl-L-α-phosphatidylcholine; PNP, 1-phenyl-3-(2-naphthyl)-2-pyrazoline; PCPP, 1-phenyl-3-(*p*-cyanophenyl)-2-pyrazoline.

2. Instrumentation

Most of the steady-state (time-averaged) excitation, emission and polarization spectra were obtained with a T-format SLM 8000 spectrofluorometer [7] (SLM Inc. Urbana, IL.) modified in our laboratory for single photon detection with Hamamatsu R928 photomultipliers. The instrument is interfaced with a PDP-11/34 computer and an *X-Y* recorder displays corrected excitation, emission and anisotropy spectra. Excitation spectra are corrected for intensity fluctuations by monitoring the excitation light intensity with a rhodamine B quantum counter whose wavelength response was determined by comparison with a rhodamine B sample in a front face cell in the sample holder [6]. To obtain corrected emission spectra, an MgO scatterer was placed in the sample position and was illuminated by a tungsten source whose temperature was determined with an optical pyrometer. Its spectral distribution was calculated from the theoretical black body spectrum for the measured temperature and was corrected for the emissivity of tungsten. It was then compared to the observed spectrum to determine the appropriate correction factors. Anisotropy spectra were corrected for imbalance between the two monochromator detector systems by use of the following formula [8].

$$\langle r \rangle = \frac{I_{VV}G - I_{VH}}{I_{VV}G + 2I_{VH}} \quad (1)$$

where

$$G = \frac{I_{HH}}{I_{HV}} \quad (2)$$

The two subscripts (V, H) of the emission intensities, I, refer to the vertical and horizontal polarization of the excitation and emission light, respectively. When necessary, the intensities of blank samples (e.g. of unlabelled cells) are subtracted from the observed intensities, e.g. $I_{VV} = I_{VV}(\text{sample}) - I_{VV}(\text{blank})$, etc.

The total fluorescence intensity, I_T, for vertically polarized excitation is

$$I_T = I_{VV} \cdot G + 2I_{VH} \quad (3)$$

the same as the denominator of Eqn. 1. After applying corrections for variations in the excitation light intensity and for sample absorbance at the excitation wavelength, quantum yields were calculated from the I_T spectra integrated over the wavelength range by using the following standards and quantum yields, ϕ: Fluorescein in 0.1 M sodium hydroxide [9]: $\phi = 0.85$; quinine bisulfate in 0.5 M sulfuric acid [10]: $\phi = 0.55$. Consistent values of ϕ were obtained when derived from both of these standards.

The absorbances of non-scattering samples were always kept below 0.1 cm^{-1} at the excitation wavelength. They were considerably higher (~1 cm^{-1}) for samples of intact red blood cells with most of this apparent absorbance being due to scattering. Such samples were measured at several titres, to ensure that the measured value of $\langle r \rangle$ was not diminished by scattering within the sample. All fluorescence measurements were performed using quartz sample cells with 3 mm × 3 mm internal cross-section.

Absorption spectra were recorded at room temperature with a Cary 17 spectrophotometer. A Sorvall superspeed RC2-B automatic refrigerated centrifuge was used for ghost and synthetic vesicles preparations. The pH of buffer solutions was measured with a Radiometer pH meter 26.

3. Synthesis of 1-phenyl-3-(2-naphthyl)-4,5-dihydro-1H-pyrazole (PNP)

This compound and 1-phenyl-3-(*p*-cyanophenyl)-2-pyrazoline (PCPP) were synthesized by condensation of the appropriate Mannich based hydrochloride with

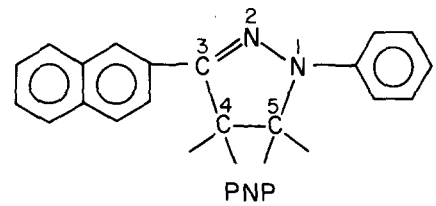

PNP

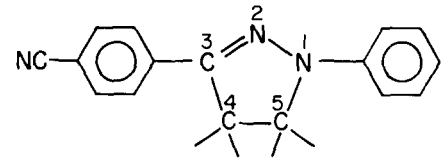

PCPP

Fig. 1. Structure of 1-phenyl-3-(2-naphthyl)-2-pyrazoline (PNP) and of 1-phenyl-3-(*p*-cyanophenyl)-2-pyrazoline (PCPP).

phenylhydrazine hydrochloride, following the procedure of Chase and Evans [11] (cf. Fig. 1). The Mannich base hydrochloride was prepared according to Maxwell [12]. The crude fluorescent probe was purified by column chromatography on alumina (activity grade I-neutral) with chloroform as eluent. This compound gave correct elemental analysis data and melted at 178°C [13].

4. Vesicle preparation

PNP-labelled phospholipid vesicles were prepared in the following manner. A concentrated chloroform solution of PNP was added to β,γ-dipalmitoyl-L-α-phosphatidylcholine (DPPC) (Calbiochem) dissolved in a minimum volume of benzene/chloroform (50 : 50, v/v). The molar phospholipid/probe ratio was about 1 000. This solution was then lyophilized to remove all traces of organic solvent. The dry powder was suspended in 50 mM KCl at 50°C and sonified under nitrogen in a glass tube with flat bottom using a Hat Systems W-350 Sonifier, operating at 70% of full power. Phosphotidylcholine concentration in this dispersion was 0.4–0.5 mM. After sonication titanium fragments released from the sonication probe were removed by centrifugation at 20 000 rev./min for 20 min at 46°C. The clear supernatant was removed with a Pasteur pipet and was used to study the temperature dependence of fluorescence polarization of the PNP. The temperature of the sample in the cuvette was measured with a copper-constantan thermocouple.

5. Ghost preparation

The method of Dodge et al. [14] was used to prepare human erythrocyte membranes. Phosphate buffer at pH 7.4 was made by mixing 0.155 M NaH_2PO_4 and 0.103 M Na_2HPO_4 solutions in the appropriate ratio. The final pH of this solution was adjusted by titration with sodium hydroxide or hydrochloric acid. This 0.105 M phosphate buffer was used to prepare a 4 mM solution at pH 7.4. All operations were performed at 4°C.

6. Labelling of ghosts

Approximately spherical glass beads (Scientific Glass Apparatus) with an average diameter of 200 μm were washed successively with concentrated nitric acid, water and ethanol and were dried overnight at 100°C. After cooling, they were mixed with a concentrated chloroform solution of the fluorescent molecule and the solvent was evaporated with continuous stirring under a gentle nitrogen stream. The coated glass beads were then dried at 60°C for 1 h. The weight percentage of the probe on the coated beads was 0.02–0.05% as determined by absorption spectroscopy of the chloroform extract of the coated beads.

A glass column with a 2–4 mm diameter was packed with the coated beads to label ghosts. About 1–2 g of coated beads were used per 10 ml of ghost suspension. The filled column was washed several times with buffer before the labelling procedure began. The temperature of the column was kept constant by circulating water through a jacket surrounding the column (cf. Fig. 3). The ghost suspension was either pumped through the column by a peristaltic pump (LKB 2115 multiperplex peristaltic pump) or was allowed to flow through the column under gravity.

Alternatively, 2 mg of PNP was dissolved in 50 ml of tetrahydrofuran, 1 ml of which was blown almost to dryness in a test-tube and taken up in 5 ml of ethanol. 10–20 μl of this solution was then added to 10 ml of an erythrocyte suspension, hematocrit 0.25%, or the equivalent ghost suspension. After centrifugation, no detectable amount of PNP was found in the supernatant.

7. Assays for labels and ghosts

The fluorescence intensity of aqueous solutions containing 2% Ammonyx-LO and the fluorophore PNP was found to be proportional to the PNP concentration. PNP taken up by ghosts or cells could be extracted with greater than 90% recovery by adding an equal volume of 4% Ammonyx-LO solution. This provided a quick and convenient assay for the PNP concentration in a sample. The efficiency of the extraction by the detergent could be estimated from the measured anisotropy of PNP in Ammonyx-LO micelles, since the anisotropy of PNP in micelles (0.077 at 450 nm) is considerably lower than the anisotropy of membrane bound PNP. This is illustrated in Fig. 2.

The titre of ghost suspensions was determined from their absorption at 280 nm in 1% SDS. Alternatively the ghost concentrations in a sample was determined

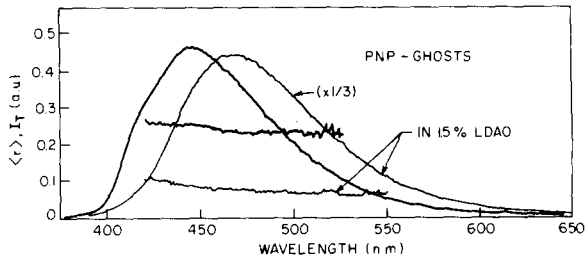

Fig. 2. The heavy lines give the fluorescence and emission anisotropy spectra of PNP-labelled ghost at 20°C where excited at 360 nm. After addition of Ammonyx-LO (final concentration 1.5%) and 30 min of incubation at room temperature, the spectra shown by the light curves were recorded. They are identical to the fluorescence and anisotropy spectra of PNP in 1.5% lauryldimethylamine-*N*-oxide. It is therefore possible to conclude that the extraction efficiency of the detergent is greater than 90%.

from its protein content [15]: 20–100 μg of ghosts were solubilized in 0.1 ml of 5% deoxycholate in 0.1 M NaOH and diluted to 0.5 ml with water. 0.5 ml of 1% $CuSO_4 \cdot 5\ H_2O$ and 0.5 ml of 2% potassium or sodium tartrate in water were mixed with 49 ml of 2% Na_2CO_3 in 0.1 M NaOH. 2.5 ml of this solution were mixed well with 0.5 ml of the ghost solution and allowed to stand for 30 min at room temperature. Then 0.25 ml of 1 M Folin reagent [16] was added and mixed very rapidly. After 30 min at room temperature, the absorption of the solution was measured at 750 nm. Standard solutions were prepared from fatty acid free human serum albumin (fraction V) (Miles Laboratories, Inc.).

III. Results

Human erythrocyte ghosts were labelled by passing them through a column packed with PNP-coated glass beads, as described in the previous section. Fig. 3 shows the number of PNP molecules per ghost as a function of the number of passes through glass bead column at various column temperatures. Although the number of embedded PNP molecules increased with the number of passes, Fig. 4 shows that the average emission anisotropy, $\langle r \rangle$, (as well as the shape of the fluorescence spectrum) is independent of this number. This suggests that the PNP environment in the membrane is independent of the number of labels per ghost. The maximum number of PNP molecules

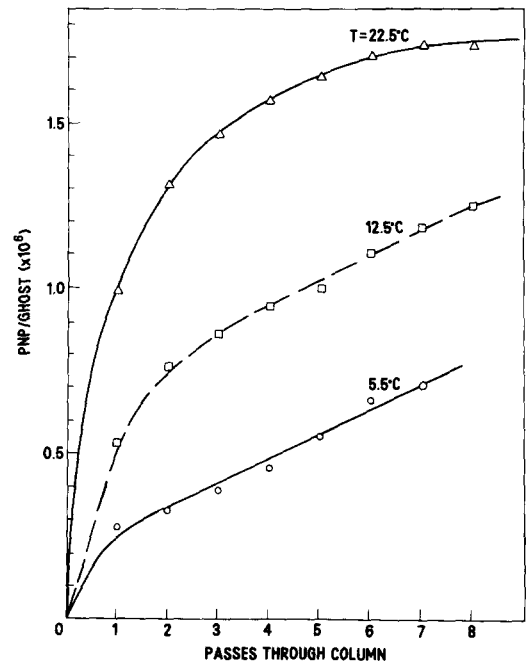

Fig. 3. The number of PNP molecules retained by erythrocyte ghosts as a function of the number of times a ghosts suspension is passed through a column of PNP-coated glass beads. The jacketed glass bead column was at the stated temperatures.

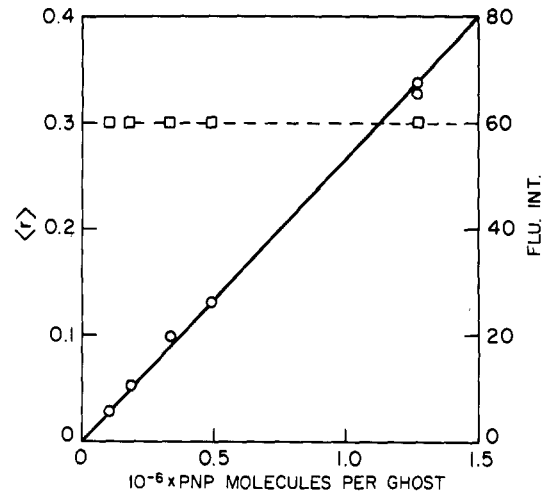

Fig. 4. The fluorescence intensity in arbitrary units and the steady state anisotropy, $\langle r \rangle$, of PNP in erythrocyte ghosts as a function of the number of PNP molecules per ghost. The temperature was 22°C. The probe's anisotropy is seen to be independent of the probe concentration.

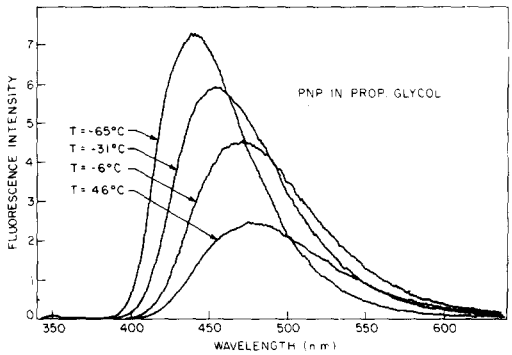

Fig. 5. Total fluorescence emission spectra of PNP in propylene glycol as a function of temperature. The excitation wavelength was 350 nm.

which can be inserted by this method is about $1.5 \cdot 10^6$ per ghost.

Like other pyrazoline derivatives which have been studied, PNP has a fluorescence spectrum which depends strongly on its environment [17]. Fig. 5 shows that the PNP spectrum in propylene glycol is also strongly temperature dependent and suggests that solvent re-orientation, which is inhibited at low temperatures, is responsible for the bathochromic shifts of PNP in hydrophylic solvents. Complete data on the relative quantum yield, anisotropy and spectral maximum of the PNP fluorescence are shown in Fig. 6. Similar data for another pyrazoline derivative, 1-phenyl-3-(*p*-cyanophenyl)-2-pyrazoline (PCPP) are shown in Fig. 7.

Fig. 8 gives the corrected excitation and emission spectra as well as the excitation and emission anisotropy spectra of PNP in propylene glycol at 0.2°C. It can be seen that $\langle r \rangle$ is almost constant over the emission band and over the lowest absorption band. The limiting anisotropy, r_0, for PNP in propylene glycol is reached at about −50°C (see Fig. 6) and is 0.385 ± 0.003. Note that the quantum yield reaches its limiting value at about the same temperature.

Unlike PNP in propylene glycol, PNP embedded in ghosts was found to have a wavelength dependent emission anisotropy spectrum. This can be seen in Fig. 2. Fig. 9 shows that the anisotropy of PNP in ghosts, averaged from 420 to 470 nm, drops from 0.298 to 0.185 as the temperature is raised from 2 to 38°C. Over the same temperature range, the slope of the emission anistropy with wavelength, $[r(440) - r(500)]/\langle r \rangle$, increases from 0.09 to 0.33. The

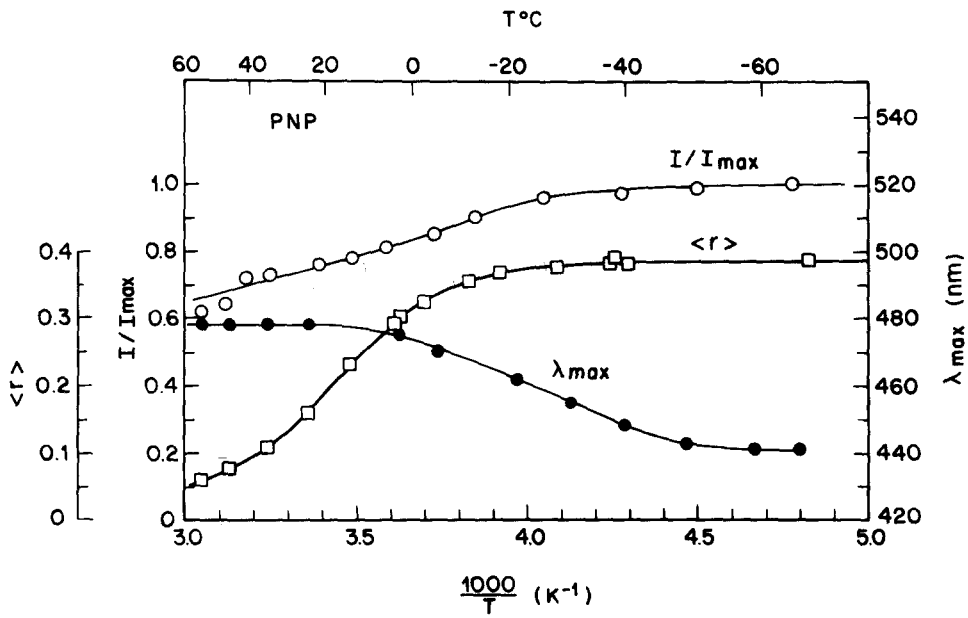

Fig. 6. The PNP steady state emission anisotropy $\langle r \rangle$, the wavelength of the maximal fluorescence intensity, λ_{max}, and the intensity, I/I_{max}, as functions of temperature. The solvent is propylene glycol. The limiting anisotropy, $r_0 = 0.385$, is seen to be reached at about −40°C. The exitation wavelength was 360.

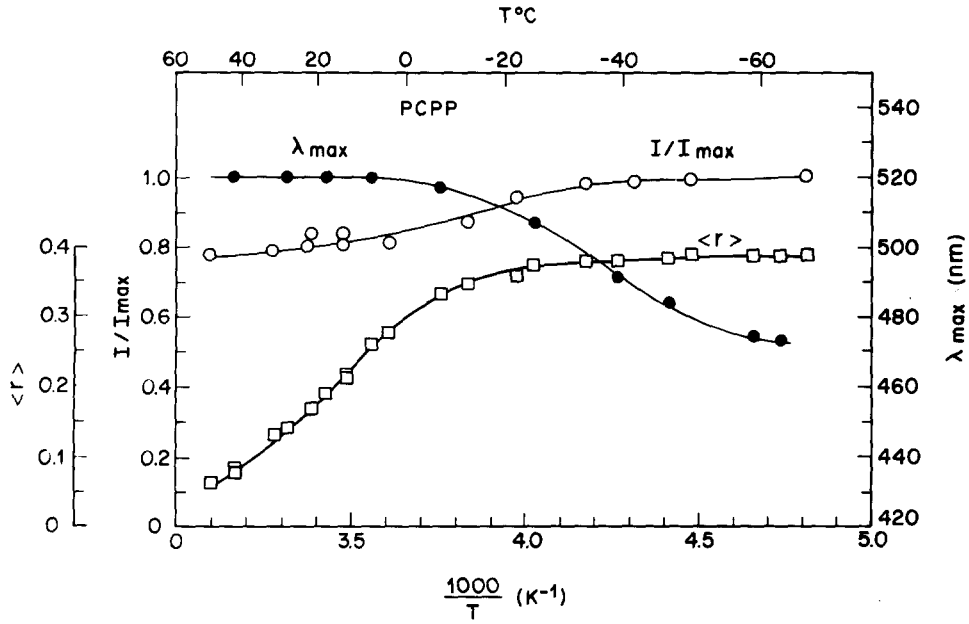

Fig. 7. The PCPP steady state emission anisotropy $\langle r \rangle$, the wavelength of the maximal fluorescence intensity, λ_{max}, and the intensity, I/I_{max}, as functions of temperature. The solvent is propylene glycol.

fluorescence intensity, on the other hand remains practically constant over this temperature range, corresponding to a quantum yield of 0.05.

Fig. 10 shows a comparison of the fluorescence spectra of PNP-labelled ghosts and intact erythrocytes. It is noteworthy that the quantum yield of PNP in intact cells, approx. 0.03, is not much smaller than for PNP in ghosts, and that (apart from a shift in

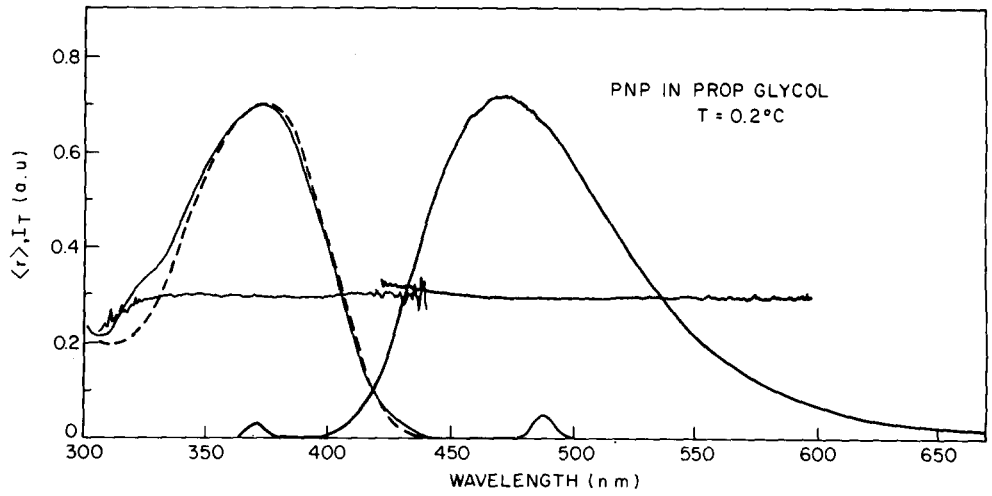

Fig. 8. The right side shows the fluorescence and anisotropy emission spectra of PNP in propylene glycol at 0.2°C. The small peak at 370 nm is due to scattered excitation light. The left side shows the corresponding fluorescence and anisotropy excitation spectra while monitoring the fluorescence at 485 nm. The dashed curve shows the PNP absorption spectrum which is seen to agree well with the excitation spectrum.

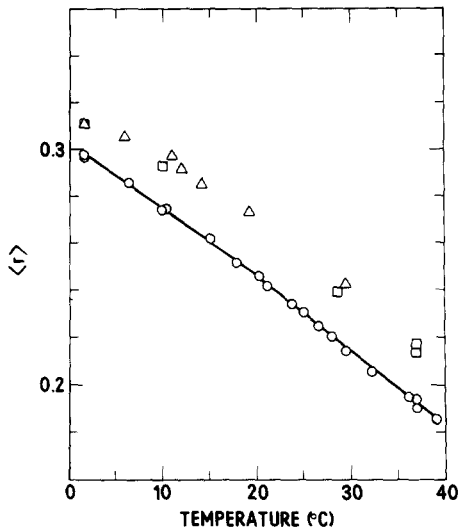

Fig. 9. The circles show the steady state anisotropy averaged between 420 and 470 nm of PNP in erythrocyte membranes as a function of temperature. The points are fitted by two straight lines which intersect at a small angle at a temperature of about 20°C. The emission anisotropy obtained for DPH in erythrocyte membranes is shown by the square symbols. The triangles are DPH anisotropy values calculated from the data given in Ref. 22.

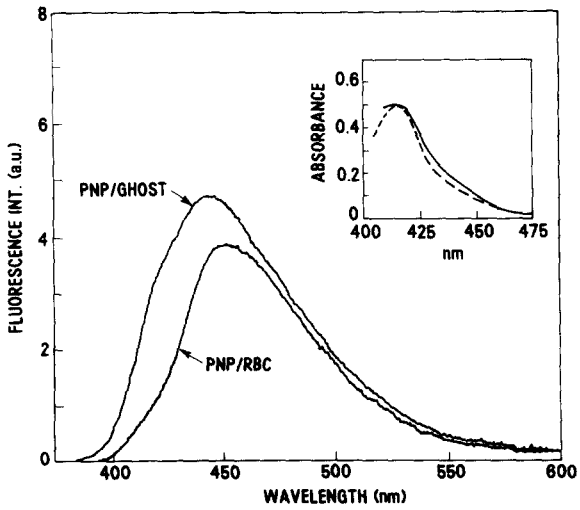

Fig. 10. Comparison of the fluorescence spectra of PNP in erythrocyte ghosts and in the membrane of intact erythrocytes. The intensity ratio between the two spectra was converted to absorbance units and shown in the insert. The dashed curve is the absorption spectrum of oxyhemoglobin in the region of the Soret band, normalized to the same peak absorbance.

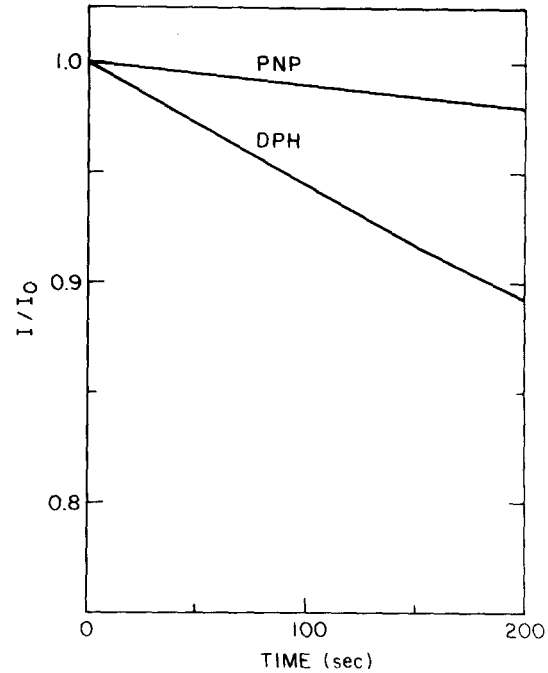

Fig. 11. The decrease of the fluorescence intensity signal with irradiation time for PNP and DPH probes embedded in erythrocyte ghosts. The irradiation wavelength was 350 nm and the temperature was 22°C. For the same excitation intensity, DPH is seen to bleach at a rate which is five times as great at the PNP bleaching rate.

the fluorescence spectrum maximum caused by absorption by the hemoglobin Soret band) it has the same fluorescence spectrum. This suggests that PNP will be a useful probe for the study of membranes of intact cells. The reduction of the quantum yield for the intact cells is due partly to the absorption mentioned above, and partly due to long range (Förster) excitation energy transfer to hemoglobin, which shortens the probe's lifetime without distorting its emission spectrum.

The most widely used reorientational probe for membrane studies is all-*trans*-1,6-diphenylhexatriene (DPH) [5,6,18–22,24,25]. This probe was found to be approx. 5-times more photolabile than PNP when irradiated in ghosts by 357 nm light (see Fig. 11). While the PNP fluorescence intensity dropped under irradiation, this did not affect the probe's anisotropy spectrum.

PNP was embedded in DPPC vesicles to test if the probe is sensitive to phospholipid phase transitions

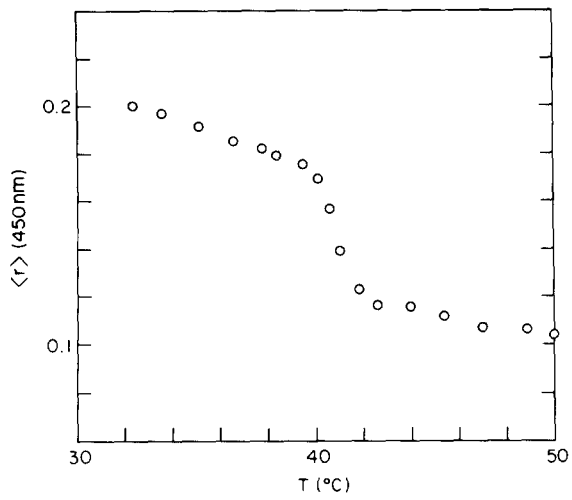

and Fig. 12 shows the steady state PNP emission anisotropy at 450 nm, as a function of temperature. No attempt was made to separate the vesicles according to size. A phase transition, about 2 degrees wide is observable at 41°C. This is the same temperature and width as were found for DPCC vesicles by the use of DPH probes [21]..

In order to gain a better understanding of the wavelength dependence of $\langle r \rangle$, the fluorescence decay of PNP-labelled ghosts was measured at two emission wavelengths, 420 and 500 nm. The data shown in Fig. 13 were obtained by means of a photon counting apparatus using 20 nm wide interference filters to define the excitation (360 nm) and emission wavelengths. The experimental decay curves were fitted with triply exponential decays of the form

$$I(t) = \sum_{i=1}^{3} \alpha_i \exp(-t/\tau_i) \tag{4}$$

after convolution with the time profile of the exciting light pulse (cf. Fig. 13). The mean lifetime, defined as

$$\langle r \rangle = \sum_{i=1}^{3} \alpha_i \tau_i \tag{5}$$

was found to be 3.6 ns and 4.7 ns at the 420 and 500 nm emission wavelengths, respectively.

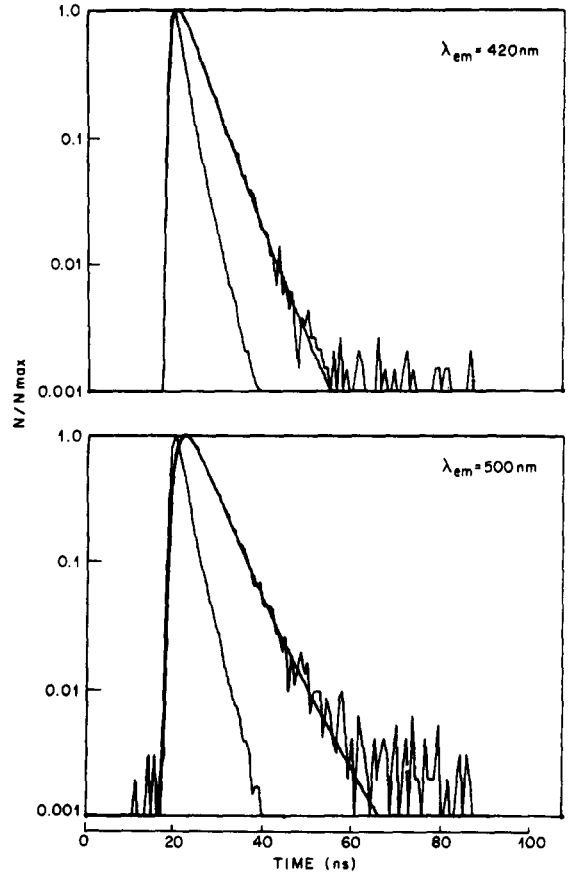

Fig. 13. The experimental (Noisy curves) decays of PNP in ghosts at 22°C, fitted with triply exponential decay functions (cf. Eqn. 4), convoluted with the time profile of the exciting light pulse (smooth curves). Two emission wavelengths, 420 and 500 nm were used. The narrow curves are the time profiles of the lamp, obtained by means of a scattering solution sample, measured at the appropriate wavelengths.

Discussion

While theoretical considerations play an important part in the design of molecular probes, the probe's usefulness depends in the final analysis on its sensitivity to the molecular environment to which it is exposed in the system under study. Pyrazoline probes, such as PNP, were investigated by us primarily as orientational probes for the study of erythrocyte and other membranes. Among their desirable spectroscopic attributes for this purpose are the following:

1. Pyrazolines have an elongated structure and their lowest excited electronic states are nondegenerate. The limiting anisotropy, r_0, of PNP is indeed very high, as is r_0 for PCPP ($r_0 \approx 0.385$ for both).

2. The Stokes' shift of PNP is large. As a result there is little overlap between the PNP absorption and emission bands and the homogeneous energy transfer, which can cause fluorescence depolarization, is negligible.

3. Since PNP fluoresces further in the red than DPH, its emission spectrum is distorted less by hemoglobin absorption ($\lambda \sim 415$ nm). Experiments in our laboratory have shown moreover, that anisotropy measurements of PNP in intact erythrocytes are feasible, since the corrected values obtained for $\langle r \rangle$ were found to be independent of the cell titre and hence of the amount of scattering [23].

4. Pyrazolines are relatively photo-stable.

Among the disadvantages of pyrazolines, their short lifetime (~4 ns) should be mentioned (De Schrijver, F.C. and Windels, C. (1979) private communication). It may limit the probe's sensitivity to molecular motion which is characterized by much longer relaxation times.

While the fluorescence anisotropy of PNP dissolved in propylene glycol is constant across its emission band (cf. Fig. 8), it decreases with increasing wavelength when it resides in phospholipid vesicles or erythrocyte membranes (cf. Fig. 2). This could arise from two causes:

1. The sites of PNP in the membrane may be heterogeneous. Solution studies [17,26] have shown that the probe's fluorescence spectrum is indeed very sensitive to its environment. The PNP sites corresponding to 'blue' emission may provide a stiffer environment (high $\langle r \rangle$) while 'red' sites are relatively more fluid (low $\langle r \rangle$).

2. The lipid enviroment of PNP in its excited state changes in a time comparable with its fluorescence lifetime, in analogy to solvent shell relaxation in the excited state. The 'late' fluorescence would then be red-shifted compared to the prompt emission, whose anisotropy would of course be the highest.

The fact that the fluorescence lifetime was found to be appreciably shorter at the shorter emission wavelength, suggests that the second explanation for the wavelength dependence of $\langle r \rangle$ is the appropriate one. A better understanding of the dynamics of PNP in the membrane could be obtained in measuring the time dependence of the probe's anisotropy.

Concerning the interpretation of the fluorescence polarization experiments, it is not possible to propose or test a model for the rotational relaxation of PNP within the membrane, from the time averaged anisotropy measurements reported here. The simplest plausible model for PNP in a phospholipid bilayer is that of a transition dipole wobbling within a cone, whose axis is normal to the phospholipid surface (isotropic hindered rotator). It has been clearly shown that time resolved fluorescence and polarization experiments are needed before the critical parameters of such a model (e.g. the rotational diffusion rate of the moment and its angular distribution) can be determined [24,25]. Such experiments are now being planned.

Qualitatively, it is clear however, that as the temperature is raised from 0 to 38°C, the anisotropy of PNP in erythrocyte ghosts drops sharply and reflects a considerable increase in the fluidity of the phospholipid regions. This in in agreement with a similar result obtained with DPH-labelled membranes [22].

Acknowledgement

N.B. thanks the N.F.W.O. (Belgium) and the Research Fund of the K.U. Leuven for financial support.

References

1 Radda, G.K. and Vanderkooi, J. (1972) Biochim. Biophys. Acta, 265, 509–549
2 Azzi, A. (1975) Q. Rev. Biophys., 8, 237–316
3 Radda, G.K. (1975) Methods in Membrane Biology, Vol. 4 (Korn, E.K., ed.), p. 97, Plenum Press, New York
4 Mantulin, W.W. and Pownall, H.J. (1977) Photochem. Photobiol. 26, 69–73
5 Shinitzky, M. and Barenholz, Y. (1978) Biochim. Biophys. Acta 515, 367–394
6 Eisinger, J. and Flores, J. (1979) Anal. Biochem. 94, 15–21
7 Jameson, D.M., Weber, G. Spencer, R.D. and Mitchell, G. (1978) Rev. Sci. Instrum. 49, 510–514
8 Chen, R.F. and Bowman, R.L. (1965) Science 147, 729–732
9 Parker, C.A. and Rees, W.T. (1960) Analyst 85, 587–600
10 Melhuish, W.H. (1961) J. Phys. Chem. 65, 229–235
11 Chase, B.H., and Evans, J.M. (1964) J. Chem. Soc., 4825–4831

12 Maxwell, C.E. (1955) Organic Syntheses, Coll. Vol. III, pp. 305–306, Wiley, New York
13 Kenner, J. and Statham, F.S. (1936) Chem. Ber. 69, 16–18
14 Dodge, J.T., Mitchell, C.V. and Hanahan, D.J. (1963) Arch. Biochem. Biophys. 100, 119–130
15 Lowry, O.H., Rosebrough, N.J., Farr, A.L. and Randall, R.J. (1951) J. Biol. Chem. 193, 265–275
16 Folin, O. and Ciocalteu, V. (1927) J. Biol. Chem. 73, 627–650
17 Strähle, H., Seitz, W. and Güsten, H. (1976) Z. Naturforsch. 31B, 1248–1255
18 Shinitzky, M. and Barenholz, Y. (1974) J. Biol. Chem. 249, 2652–2657
19 Shinitzky, M. and Inbar, M. (1974) J. Mol. Biol. 85, 603–615
20 Cehelnik, E.D., Cundall, R.B., Lockwood, R. and Palmer, T.F. (1975) J. Phys. Chem. 79, 1369–1376
21 Suurkuusk, J., Lentz, B.R. Barenholz, Y., Biltonen, R.L. and Thompson, T.E. (1976) Biochemistry 15, 1393–1401
22 Aloni, B., Shinitzky, M. and Lione, A. (1974) Biochim. Biophys. Acta 348, 438–441
23 Eisinger, J. and Flores, J. (1981) manuscript in preparation
24 Chen, L.A., Dale, R.E., Roth, S. and Brand, L. (1977) J. Biol. Chem. 252, 2163–2169
25 Lakowicz, J.R., Prendergast, F.G. and Hogen, D. (1979) Biochemistry 18, 508–519
26 Windels, C. (1979) Het Gebruik van Pyrazoline-Derivaten als Fluorescentiesondes, Thesis, Katholieke Universiteit, Leuven, Faculty of Science